W physics at the ILC with polarized beams as a probe of the Littlest Higgs model

B. Ananthanarayan,[a] **Monalisa Patra**[a] **and P. Poulose**[b]

[a] *Centre for High Energy Physics, Indian Institute of Science,*
Bangalore 560 012, India

[b] *Department of Physics, Indian Institute of Technology Guwahati,*
Guwahati 781 039, India

E-mail: anant@cts.iisc.ernet.in, monalisa@cts.iisc.ernet.in,
poulose@iitg.ernet.in

ABSTRACT: We study the possibility of using W pair production and leptonic decay of one of the W's at the ILC with polarized beams as a probe of the Littlest Higgs Model. We consider cross-sections, polarization fractions of the W's, leptonic decay energy and angular distributions, and left-right polarization asymmetry as probes of the model. With parameter values allowed by present experimental constraints detectable effects on these observables at typical ILC energies of 500 GeV and 800 GeV will be present. Beam polarization is further found to enhance the sensitivity.

Contents

1 Introduction

One of the important processes that will be studied at high precision at ILC with and without beam polarization is W-pair production. Phenomelonogical studies of this process within the Standard Model (SM) have been carried out in great detail [1, 2]. Since properties of the weak gauge bosons are closely linked to electroweak symmetry breaking (EWSB) and the structure of the gauge sector in general, detailed study of W physics will throw light on what lies beyond the SM. The study of mechanisms of EWSB is one of the main concerns of particle physics today. The standard Higgs mechanism is less than satisfactory, and faces difficulties such as the hierarchy problem. Looking beyond the SM, the newly proposed Little Higgs scenarios [3, 4] provide a dynamical way to generate the EWSB, in contrast to the *ad hoc* introduction of the elementary scalar sector. Apart from this aesthetically appealing feature, provide rich phenomenology with predictions that could be vidicated or ruled out at future colliders such as the LHC and the ILC.

One major feature of such models is the presence of additional gauge bosons in the physical spectrum. These influence processes like W-pair production in e^+e^- collisions, firstly directly through their exchange in the process, and secondly through the change of standard couplings through mixing with other gauge bosons. Although these additional gauge bosons are typically too heavy to be produced at reference ILC energies of 500 and 800 GeV which we use in the present study, their effects manifest themselves as stated above. Recently it was pointed out, in a preliminary study, that for one such model known as the Littlest Higgs Model (LHM), the fraction of longitudinally and transversely polarized of one of the W's could be significantly different from the corresponding fraction

in the SM [5]. In this work, we consider a refined treatment of the LHM to be described below, and extend the prior work to polarization fractions and total cross-sections of the W's, energy and angular distributions of decay leptons, as well as to observables like the forward-backward and left-right asymmetries, which are more sensitive to the effects of the LHM compared to the cross-sections.

The ILC is expected to have large beam polarizations which will significantly enhance the sensitivity to new physics, for a review, see ref. [6]. We consider different beam polarizations with the aim of improving the sensitivity of the observables considered here.

This article is organized as follows: in section 2 we, very briefly, introduce the LHM, and describe its particle spectrum and couplings relevant to $e^+e^- \to W^+W^-$. In section 3 we present our analysis of the total cross section and W-polarization fractions in the LHM and compare with the SM case. In section 4 we take up the task of probing the model by considering decay of one of the $W's$ to a lepton pair. We consider the energy and angular distributions for the cases of SM and LHM. We also discuss the left-right as well as forward-backward asymmetry in this section. Finally we summarize our study and present our conclusions in section 5. Note that we have included beam polarization effects in this study in each of the relevant sections.

2 The Littlest Higgs model and W pair production at ILC

In Little Higgs models [3] a non-linear realization of some global symmetry G broken down to H is considered. The Nambu-Goldstone Bosons (NGB) of the symmetry breaking are candidate Higgs fields. In a specific model, called LHM [4] $G \equiv \mathrm{SU}(5)$ is broken down to $H \equiv \mathrm{SO}(5)$ via a vacuum expectation value (vev) of order f. Interactions of NGB's are described by a non-linear sigma model, which is an effective theory valid below the cut off $\Lambda \sim 4\pi f$. In the version of the LHM [4, 7, 8] we will consider in this report, $\mathrm{SU}_1(2) \times \mathrm{SU}_2(2) \times \mathrm{U}_Y(1) \subset \mathrm{SU}(5)$ is gauged, which is broken down to the SM gauge group $\mathrm{SU}(2)_L \times \mathrm{U}(1)_Y$. Under this, the 14 NGB's transform as a real singlet, a real triplet, a complex doublet and a complex triplet. The real fields become the longitudinal degrees of the heavy gauge bosons, while the SM gauge bosons, $\vec{W}_L^\mu$ and B_L^μ remain massless at this stage. The doublet NGB field has the correct quantum numbers to be identified as the standard Higgs doublet. At tree level, they have only derivative couplings, but quantum corrections at one-loop level generate a Coleman-Weinberg potential with quadratic and quartic terms, consequently breaking electroweak symmetry. Gauge symmetry is constructed such that, in the absence of any one (original) gauge interaction the Higgs is massless to all orders. This also ensures that quadratically divergent contributions to the mass-square term at one-loop level are cancelled between the gauge bosons from the two sectors. Logarithmically divergent terms contribute to the potential. In order to avoid a quadratic divergence due to a top-quark loop, a pair of (weak-singlet) Weyl quarks U_L, U_R is introduced, which mix with the ordinary left- and right- quarks to give mass eigenstates. Here again, it is so arranged such that the quadratic divergence coming from the standard top-quark is cancelled by its heavy counterpart, and the logarithmically divergent part is added to the Coleman-Weinberg potential. The model achieves EWSB, at the same time, protecting the Higgs mass from accquiring quadratically divergent corrections at one loop.
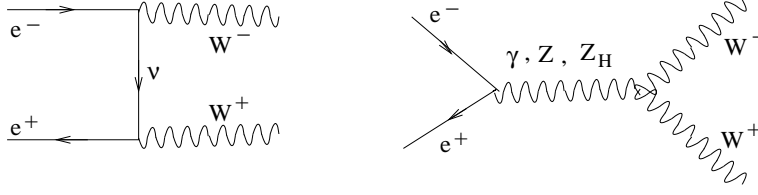
Figure 1. Feynman diagrams contributing to the process $e^-e^+ \to W^+W^-$ in the LHM.

It is therefore to be expected that these models will have a rich phenomenology with distinct signatures that can be probed at upcoming collider experiments. An incomplete list of phenomenological studies of different variations of the Little Higgs Model scenarios is ref. [8–11].

Our interest here is the effective theory below the cut-off Λ. For the process $e^+e^- \to W^+W^-$, we have an $s-$channel process with the exchange of the heavy neutral gauge boson, Z_H, in addition to the standard channels as shown in figure 1.

Apart from the contribution due to the additional s-channel process, the LHM also changes the SM couplings. The relevant couplings in terms of the parameters of the LHM is given below in terms of the global symmetry breaking scale f, the parameter $\cos\theta$, which represents mixing between the two gauge sectors of the LHM and the vev.

The three-point gauge couplings involving WW are given by:

$$V^\mu(k_1)W^\nu(k_2)W^\rho(k_3) = ig_{\mathrm{VWW}}\ [g^{\mu\nu}(k_1 - k_2)^\rho + g^{\nu\rho}(k_2 - k_3)^\mu + g^{\rho\mu}(k_3 - k_1)^\nu],$$

where all the momenta are considered outflowing, and $V \equiv \gamma,\ Z,\ Z_H$. Individual g_{VWW} are given by:

$$g_{\gamma WW} = -e \tag{2.1}$$

$$g_{\mathrm{ZWW}} = -e\ \frac{\cos\theta_W}{\sin\theta_W} \tag{2.2}$$

$$g_{Z_H WW} = \frac{ev^2}{8f^2 \sin\theta_W}\ \sin 4\theta \tag{2.3}$$

Fermion couplings are given by:

$$g_{e\nu W} = i\frac{g}{2\sqrt{2}} \left[1 - \frac{v^2}{2f^2}\cos^2\theta\cos 2\theta\right]\ \gamma^\mu\ (1 - \gamma^5) \tag{2.4}$$

$$g_{\mathrm{eeV}} = i\gamma^\mu(c_V^v - c_V^a\gamma^5), \tag{2.5}$$

where

$$c_\gamma^v = -e; \qquad c_\gamma^a = 0 \tag{2.6}$$

$$c_Z^v = -\frac{e}{\sin 2\theta_W}\left[\left(-\frac{1}{2} + 2\sin^2\theta_W\right) - \frac{v^2}{f^2}\frac{\sin 4\theta\cot\theta}{2}\right] \tag{2.7}$$

$$c_Z^a = -\frac{e}{\sin 2\theta_W}\left[-\frac{1}{2} - \frac{v^2}{f^2}\frac{\sin 4\theta\cot\theta}{2}\right] \tag{2.8}$$

$$c_{Z_H}^v = c_{Z_H}^a = -\left(\frac{e\cot\theta}{4\sin\theta_W}\right) \tag{2.9}$$

Following ref. [10] we consider the measured values of the Fermi coupling constant, G_F, the Z-boson mass, M_Z, and the fine structure constant, $\alpha_{\text{em}}(M_Z^2)$ as the Standard Model input parameters. The weak mixing angle is obtained from the relation:

$$\sin^2 \theta_0 \ \cos^2 \theta_0 = \frac{\pi \alpha_{\text{em}}(M_Z^2)}{\sqrt{2} G_F M_Z^2}$$

.

The bare weak mixing angle, θ_W is related to the measured weak coupling angle, θ_0 through the following relation:

$$\cos \theta_W = \cos \theta_0 \left[1 + \frac{\sin^2 \theta_0}{\cos^2 \theta_0 - \sin^2 \theta_0} \left(\frac{v^2 \cos^2 \theta \sin^2 \theta}{2f^2} + 2 \frac{|v'|^2}{v^2} \right) \right]$$

The weak coupling constant expressed in terms of the other parameters becomes

$$g = \frac{2m_W}{v} \left[1 + \frac{v^2}{2f^2} \left(\frac{1}{6} + \frac{(\cos^2 \theta - \sin^2 \theta)^2}{4} \right) - 2 \frac{|v'|^2}{v^2} \right].$$

The triplet vev, v' is related to the generated quartic coupling, and the guage couplings through

$$\frac{|v'|^2}{v^2} = \frac{v^2}{144f^2} \left(1 + \frac{6\lambda - 4ag_1^2}{a(2g'^2 + g_1^2)} \right)^2,$$

which is further constrained to $|v'|^2/v^2 < v^2/16f^2$ [8]. In our numerical analysis we consider the approximate relation, $|v'|^2/v^2 = v^2/144f^2$. Note that our numerical results are not very sensitive to this choice. Thus we are left with two free parameters f and θ. As argued by [11], precision electroweak measurements restrict the parameters to be $f \sim 1\,\text{TeV}$ and $0.1 < \cos\theta < 0.9$. In our numerical analysis we consider some representative values satisfying these restrictions.

3 Analyses of $e^- e^+ \to W^+ W^-$

In this section we present the results of our numerical analysis to probe the LHM through the process $e^- e^+ \to W^+ W^-$ at the ILC.

3.1 The total cross section

We compute the total cross section incorporating beam polarization using the helicity amplitudes given in ref. [1] with the new couplings and with the added contribution due to the exchange of Z_H. With beam polarization, in general, the polarized cross section may be expressed as [12]:

$$\sigma(e^+ e^- \to W^+ W^-) = \frac{1}{4} \big[(1 + P_{e^-}).(1 - P_{e^+}) \sigma^{RL} \\ + (1 - P_{e^-}).(1 + P_{e^+}) \sigma^{LR} \big], \qquad (3.1)$$

where $\sigma^{RL} = \sigma(e_L^+ e_R^- \to W^+ W^-)$ and $\sigma^{LR} = \sigma(e_R^+ e_L^- \to W^+ W^-)$, with $e_{L,R}$ representing the left- and right-polarized electrons (and positrons), respectively. The degree of polarization is defined as: $P_e = (N_R - N_L)/(N_R + N_L)$, where $N_{L,R}$ denote the number of
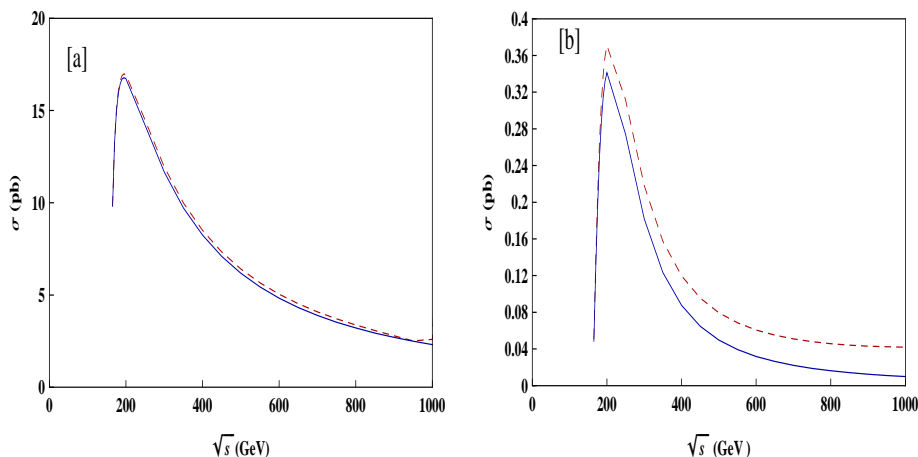
Figure 2. Total cross section for $W^+ W^-$ production in an e^+e^- collision for SM [blue-solid] and LHM [red-dashed] with [a] unpolarized beams [b] polarized beams with $P_{e^-}=1$ and $P_{e^+}=0$. The parametres for LHM are $f=1\,\text{TeV}$ and $c=0.3$

left-polarized and right-polarized electrons (and positrons), respectively. More than 80% of electron beam polarization and large positron beam polarization are expected to be achieved at ILC. In our analysis we consider the ideal possibility of 100% polarization of the beams. Our results are presented in the figures.

In figure 2 we present the total production cross-section for a typical choice of parameters of the LHM and in the SM for the case of unpolarized and polarized beams with a specific choice of beam polarization. It may be seen that in the case of unpolarized beams the cross section of LHM does not deviate much from that of the SM for energies up to 1 TeV.

The presence of beam polarization changes this situation significantly. The combination, $P_{e^-} = +1$ and $P_{e^+} = 0$ is seen to provide the largest deviation, which is the case we have chosen to display. However, for this configuration a reduced number of W-pairs is produced, as the dominant t-channel is cut off. Notice also that there is no contribution due to the Z_H exchange in this case, as the Z_H couples only to the left-handed electrons. The effect, therefore is purely due to the deviation of the standard model couplings. We will return to some more properties of this in the next sub-section.

3.2 W polarization fractions

Here we explore the sensitivity of the ILC to the LHM when we consider polarization fractions of the W bosons. Such measurements have been considered in past experiments for precision studies of the W boson properties at LEP, which has measured the fractional cross section of the polarized W's [13]. At ILC higher precision is expected to be reached. We define the polarization fractions as

$$f^0 \equiv \sigma(e^+e^- \to W_L^- W^+)/\sigma_{\text{unpol}} \tag{3.2}$$

$$f^T \equiv \sigma(e^+e^- \to W_T^- W^+)/\sigma_{\text{unpol}}, \tag{3.3}$$

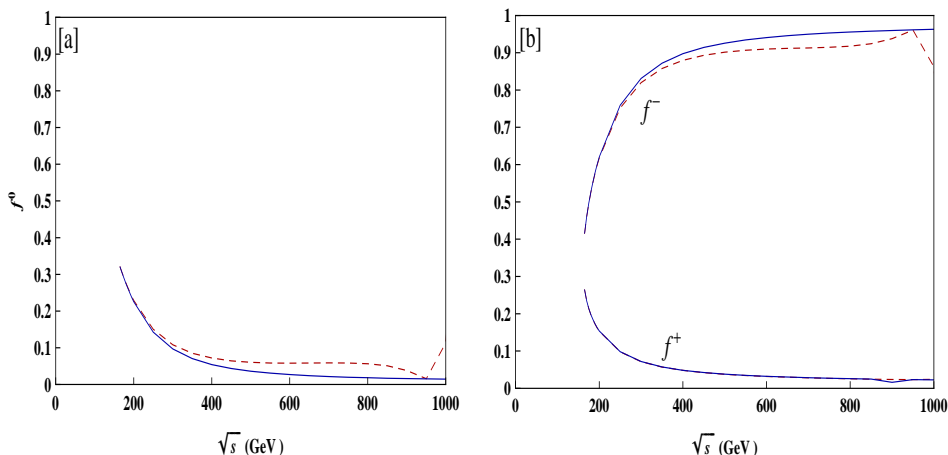where L stands for longitudinal polarization, and $T = \pm$ stands for transverse polarizations.

Figure 3. Fractional cross section of W^-, [a] longitudinal (f^0), and [b] transverse ($f^\pm$), with unpolarised beams for SM [blue - solid] and LHM [red - dashed]. The parametres in this case are f=1 TeV and c=0.3

The three polarization fractions are studied as a function of $\sqrt{s}$ which are plotted in figure 3. It is readily observed that there is a significant deviation in the case of f^0 and f^-, while f^+ is largely unaffected. Since these fractions depend on various couplings in a complicated way, we do not attempt to explain the effects in terms of the changes in the couplings.

In table 1 we present firstly the ratio of the cross section in the LHM to that in the SM for typical parameter choices, as well as the ratio of f^0 in LHM to that in the SM at $\sqrt{s} = 500$ GeV and 800 GeV for the two illustrative parameter space points. At $\sqrt{s}$=500 GeV for f=1 TeV and c=0.3 the deviation is about 65% with unpolarized beams. This is improved marginally to about 66% for $P_{e^-} = -1$, $P_{e^+} = 0$. While for the slightly larger value of, $f = 1.5$ TeV, the effect is not as dramatic, we still have significant deviation of about 25 - 30% in f^0. On the other hand, the configuration with purely right handed electrons and unpolarized positrons has the effect of completely washing out the effect of the LHM in the polarization fractions. Therefore, beam polarization has the dramatic effect of disentangling the effects of the new physics. Crucially, there is an interplay between the pure left-handed coupling nature of Z_H and the corrections to the couplings of the SM Z-boson coming from the parameters of the LHM which makes this possible. Considering the precision at which f^0 could be measured at ILC, such effects are very interesting.

3.3 Angular spectrum of the secondary lepton

In order to exploit further the process at hand, it is profitable to consider the decays of one or both the W's. Let us consider $e^+e^- \rightarrow W^+W^-$ with $W^- \rightarrow l^-\bar{\nu}$ and W^+ going into anything. Energy-angle correlation of the secondary leptons is given by the following

P_{e^-}	P_{e^+}	f (TeV)	c	$\sqrt{s}=500\text{GeV}$		$\sqrt{s}=800\text{GeV}$	
				$\sigma_{\text{LHM}}/\sigma_{\text{SM}}$	$f^0_{\text{LHM}}/f^0_{\text{SM}}$	$\sigma_{\text{LHM}}/\sigma_{\text{SM}}$	$f^0_{\text{LHM}}/f^0_{\text{SM}}$
0	0	1	0.3	1.04	1.65	1.05	3.01
		1.5	0.3	1.02	1.27	1.03	2.06
		1.5	0.5	1.00	1.25	1.00	1.72
-1	0	1	0.3	1.04	1.66	1.05	3.08
		1.5	0.3	1.01	1.28	1.02	2.12
		1.5	0.5	1.00	1.26	1.00	1.75
+1	0	1	0.3	1.60	1.00	2.81	1.00
		1.5	0.3	1.25	1.00	1.69	1.00
		1.5	0.5	1.17	1.00	1.46	1.00

Table 1. Ratios of the cross section and W polarization fractions in the LHM to those in the SM for different beam polarizations, and for some illustrative values of f and c.

expression [14, 15]:

$$\frac{d\sigma}{dx\, d\cos\theta_l} = \frac{3}{2}\frac{\alpha^2}{s}\, BR(W^- \to e^-\bar{\nu})\, A(s,x,\theta_l)$$
$$\times \left[\arctan\left(\frac{m_W}{\Gamma_W}\right) + \arctan\left(\frac{sx}{m_W\Gamma_W} - \frac{s\tau}{m_W\Gamma_W(1-x)}\right)\right]. \quad (3.4)$$

Expression for the function $A(s,x,\theta_l)$ is given in the appendix for arbitrary beam polarization, while in the above $x = 2E_l/\sqrt{s}$, where E_l is the energy of the secondary lepton in the e^+e^- centre of mass frame with $\sqrt{s}$ the centre of mass energy, and θ_l is its polar angle. $BR(W^- \to e^-\bar{\nu})$ is the leptonic branching ratio of W, Γ_W is its width, and $\tau = m_W^2/s$. In principle, the decay width and branching ratios of W can be different from those of the SM values. But, in the case when the additional fermions are heavy, we can assume an SM like decay of the W. In our analysis we have taken this approach.

From the above energy-angle correlation, we obtain the $\cos\theta_l$ distribution by numerically integrating over x. Figure 4 shows the angular distribution for different polarization combinations for $\sqrt{s} = 800\,\text{GeV}$. It may be noted that the θ_l distribution closely follow the pattern of the angular distribution of the W, which is expected to peak in the forward region for unpolarized beams and with left-polarized electron beams, but is symmetric in the case of right-polarized electron beams. This is expected as the W is produced with large kinetic energy, and the decay leptons are expected to follow its momentum direction. The case of right-handed electron beam figure 4(c) is interesting. Recall that Z_H couples only to the left-handed electrons. Therefore, there is no contribution from the Z_H exchange when we have right-polarized electron beam. But, we still notice appreciable deviation in the angular distribution compared to the SM case. This comes about through the change in the SM couplings. Similar effect was seen in the case of total cross section also. In the
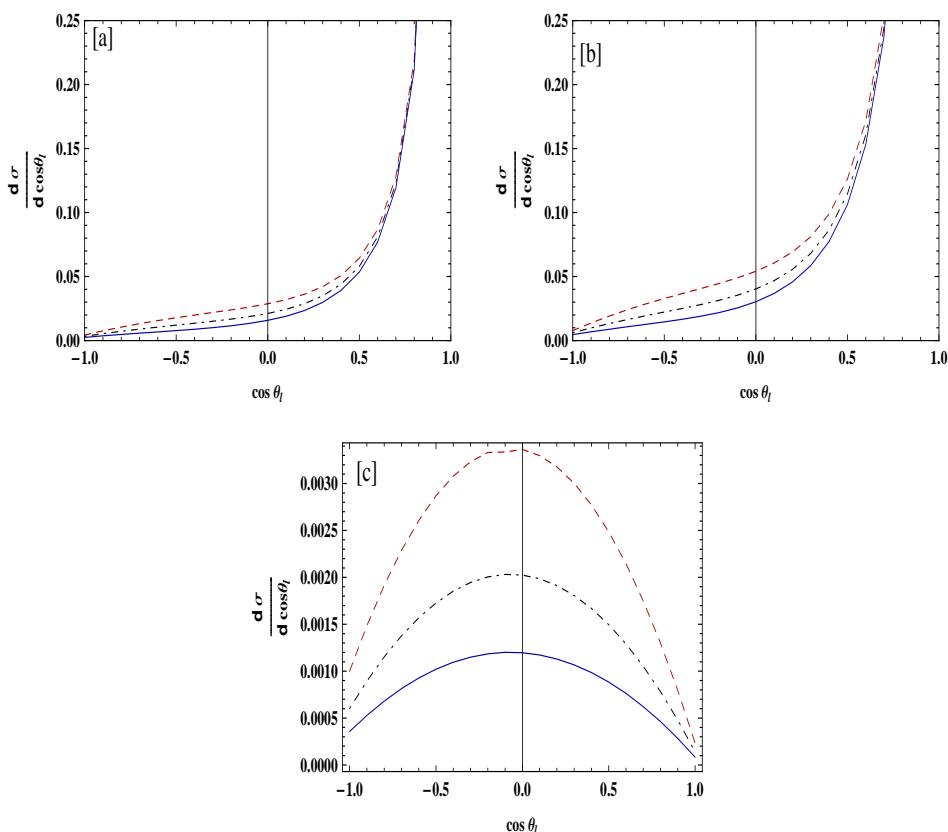
Figure 4. Angular distribution of secondary leptons at $\sqrt{s}$=800 GeV within SM [blue - solid] and LHM with f=1 TeV, c=0.3 [red - dashed] and with f=1.5 TeV, c=0.3 [black - dot-dashed] for [a] unpolarized beams, [b] with P_{e^-}=-1 and P_{e^+}=0, and [c] with P_{e^-}= 1 and P_{e^+}=0

case of $\sqrt{s} = 500$ GeV the effect is similar, but somewhat less pronounced and therefore not displayed here explicitly.

A useful quantity to obtain in the case of unpolarized and left-polarized beams is the fraction of leptons emitted in the backward direction, which may be defined as:

$$f_{\text{back}} = \frac{\int_{-1}^{0} (d\sigma/d\cos\theta_l) \ d\cos\theta_l}{\int_{-1}^{1} (d\sigma/d\cos\theta_l) \ d\cos\theta_l}$$

In table 2 we present these fractions for $\sqrt{s} = 500$ GeV, and 800 GeV. The deviation is about 34 % at $\sqrt{s}$ =500 GeV for f=1TeV and c=0.3 with unpolarised beams. Notice that the effect is not very sensitive to the choice of c. But larger f values tend to reduce the effect drastically. Using left-polarized electron beam ($P_{e^-} = -1$) does not affect the above results significantly. At $\sqrt{s} = 800$ GeV, the effects are even more dramatic, as can be judged from the table. In the case of right-polarized electron beam ($P_{e^-} = +1$), f_{back} remains the same in both LHM as well as SM.

P_{e^-}	P_{e^+}	Model	f (TeV)	c	$\sqrt{s}=500\mathrm{GeV}$		$\sqrt{s}=800\mathrm{GeV}$	
					f_{back}	A_{FB}	f_{back}	A_{FB}
0	0	SM			0.035	-0.93	0.024	-0.95
		LHM	1	0.3	0.047	-0.91	0.047	-0.91
			1.5	0.3	0.040	-0.92	0.034	-0.93
			1.5	0.5	0.039	-0.92	0.032	-0.94
-1	0	SM			0.032	-0.94	0.022	-0.96
		LHM	1	0.3	0.044	-0.91	0.044	-0.91
			1.5	0.3	0.037	-0.93	0.032	-0.94
			1.5	0.5	0.037	-0.93	0.030	-0.94

Table 2. Fraction of leptons emitted in the backward direction, and the forward-backward asymmetry for both LHM and SM model for unpolarized and polarized beams with different choices of parameters.

Another useful observable related to the angular asymmetry is the forward-backward asymmetry defined as:

$$A_{\mathrm{FB}} = \frac{\int_{-1}^{0}(d\sigma/d\cos\theta_l)\ d\cos\theta_l - \int_{0}^{1}(d\sigma/d\cos\theta_l)\ d\cos\theta_l}{\int_{-1}^{1}(d\sigma/d\cos\theta_l)\ d\cos\theta_l}. \tag{3.5}$$

In table 2 A_{FB} is tabulated for different parameter values at two different collider energies. Deviation of about 5% is observed in the asymmetry for $f = 1\,\mathrm{TeV}$ and $c = 0.3$.

3.4 Energy spectrum of the secondary lepton

The energy spectrum of the secondary leptons are sensitive to the $W^{\pm}$ helicities. The energy distribution in the centre of mass frame may be written in terms of the polarization fractions of the W's in the following form [15]:

$$\frac{1}{\sigma}\frac{d\sigma}{dx} = \frac{2}{\beta^3}\left[\frac{3}{4}f^0(\beta^2-(1-2x)^2)\right.$$
$$\left.+\frac{3}{8}f^+(\beta-1+2x)^2+\frac{3}{8}f^-(\beta+1-2x)^2\right]. \tag{3.6}$$

In figure 5 we present the energy spectrum of the charged decay lepton for $\sqrt{s} = 800\,\mathrm{GeV}$. We notice that a slightly larger fraction of hard leptons are produced in the case of LHM compared to the case of the SM. The effect is much smaller in the case of $\sqrt{s} = 500\,\mathrm{GeV}$. While it is true that the effect is not dramatic, given the fact that the lepton energy spectrum could be obtained easily and with high efficiency, this observable might be useful in probing the LHM.
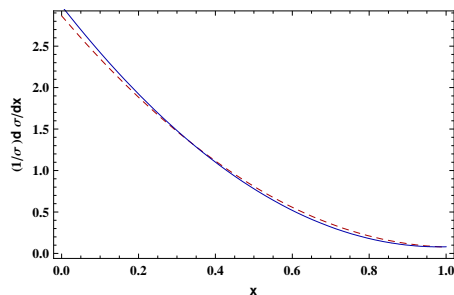
Figure 5. The energy spectrum of the charged decay lepton in $e^+e^- \to W^+W^-$, with $W^- \to l^-\bar{\nu}$ at $\sqrt{s}$=800 GeV. Unpolarised beams are used for SM [blue - solid] and LHM [red - dashed]. The parametres in this case are f=1 TeV and c=0.3
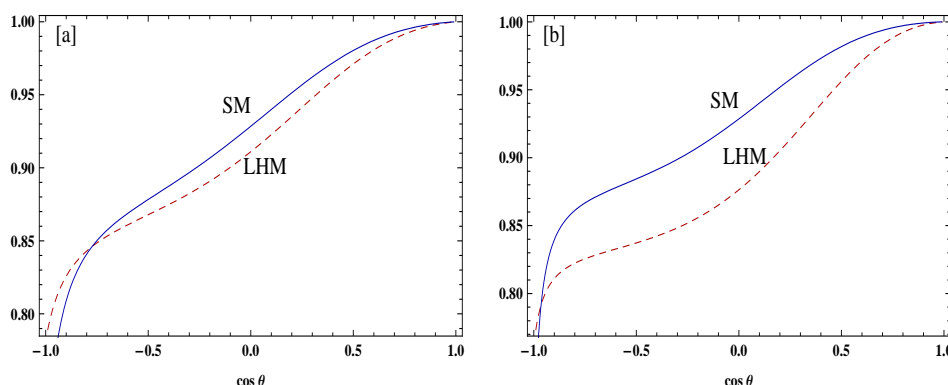

Figure 6. The left-right asymmetry for SM [blue - solid] and LHM [red - dashed] at [a]$\sqrt{s}$=500GeV [b]$\sqrt{s}$=800GeV. The parametres considered are $f = 1$ TeV and $c = 0.3$.

3.5 Left-right asymmetry

The new gauge boson Z_H in the LHM has the peculiar property of coupling only to left handed fermions as mentioned earlier. On the other hand, the SM Z couples to both left- and right- handed fermions, but the corrections to the Ze^+e^- coupling is such that only the left-handed electron coupling is affected. Thus, one would expect appreciable change in the asymmetry between the left- and right-polarized cross sectionos.

We define the left-right asymmetry in the differential cross section as:

$$A_{LR}^{\text{diff}} = \frac{(d\sigma(e_L^- e_R^+)/d\cos\theta - d\sigma(e_R^- e_L^+)/d\cos\theta)}{(d\sigma(e_L^- e_R^+)/d\cos\theta + d\sigma(e_R^- e_L^+)/d\cos\theta)}, \tag{3.7}$$

where θ is the W scattering angle. Figure 6 shows the LR asymmetry for two energies. Even at low energies the deviation becomes apparent.

We may go one step further by considering an integral version of this asymmetry as better efficiency may be obtained this way, by integrating each of the differential cross sections from an opening angle θ_0 up to an angle $\pi - \theta_0$, for various realistic values of θ_0 to which the data can be integrated without difficulty. We define the integrated left-right

Model	f (TeV)	c	A_{LR}	
			$\sqrt{s} = 500\text{GeV}$	$\sqrt{s} = 800\text{GeV}$

$\theta_0 = 0$

Model	f (TeV)	c	$\sqrt{s} = 500\text{GeV}$	$\sqrt{s} = 800\text{GeV}$
SM			0.992	0.995
LHM	1	0.3	0.988	0.986
	1.5	0.3	0.990	0.992
	1.5	0.5	0.991	0.993

$\theta_0 = 15^o$

Model	f (TeV)	c	$\sqrt{s} = 500\text{GeV}$	$\sqrt{s} = 800\text{GeV}$
SM			0.985	0.987
LHM	1	0.3	0.978	0.967
	1.5	0.3	0.982	0.979
	1.5	0.5	0.983	0.981

$\theta_0 = 30^o$

Model	f (TeV)	c	$\sqrt{s} = 500\text{GeV}$	$\sqrt{s} = 800\text{GeV}$
SM			0.974	0.976
LHM	1	0.3	0.962	0.945
	1.5	0.3	0.969	0.964
	1.5	0.5	0.970	0.967

$\theta_0 = 45^o$

Model	f (TeV)	c	$\sqrt{s} = 500\text{GeV}$	$\sqrt{s} = 800\text{GeV}$
SM			0.960	0.962
LHM	1	0.3	0.945	0.920
	1.5	0.3	0.953	0.945
	1.5	0.5	0.955	0.949

$\theta_0 = 60^o$

Model	f (TeV)	c	$\sqrt{s} = 500\text{GeV}$	$\sqrt{s} = 800\text{GeV}$
SM			0.944	0.946
LHM	1	0.3	0.927	0.897
	1.5	0.3	0.937	0.926
	1.5	0.5	0.939	0.931

Table 3. A_{LR} for various opening angles θ_0 for SM and LHM with different choice of parameters.

asymmetry as:

$$A_{LR} = \frac{\sigma_{\theta_0}(e_L^- e_R^+ \to W^+ W^-) - \sigma_{\theta_0}(e_R^- e_L^+ \to W^+ W^-)}{\sigma_{\theta_0}(e_L^- e_R^+ \to W^+ W^-) + \sigma_{\theta_0}(e_R^- e_L^+ \to W^+ W^-)} \tag{3.8}$$

where σ_{θ_0} stands for $\int_{\theta_0}^{\pi - \theta_0} d\theta \, (d\sigma/d\theta)$. This asymmetry, for different parameter values at $\sqrt{s} = 500\,\text{GeV}$ and at $\sqrt{s} = 800\,\text{GeV}$ is tabulated in table 3. We see that the asymmetry is not affected in any significant way at $\sqrt{s} = 500\,\text{GeV}$ or at $\sqrt{s} = 800\,\text{GeV}$ for the parameter

combinations considered, when no cut on angle is applied. Interesting patterns may be observed from this table. An interplay between the differential asymmetry plotted above, and the fact that the bulk of the contribution to the cross section comes from the forward region where the asymmetry itself is not appreciable leads to more sigificant results when the cut-off angle is larger. In other words, as the cut-off angle increases, the region of deviation between the LHM and the SM is weighted more efficiently. The case of $\theta_0 = 15^o$ is worthy of note, as there is a cross-over in the asymmetry for $\sqrt{s} = 800\,\text{GeV}$ and the effect is completely wiped out.

4 Conclusions

Understanding the phenomenon of electroweak symmetry breaking is central to the study of elementary particle physics. Among the viable alternatives to the Standard Higgs Mechanism is the Little Higgs Scenarios, which provides a natural way to dynamically generate electroweak symmetry breaking. In this report we have considered the LHM which is one simple version of this scenario. Such a model predicts the existence of additional gauge bosons with masses in the TeV region. We have considered the process $e^+e^- \rightarrow W^+W^-$ to probe this model. Presence of a heavy neutral gauge boson in addition to the SM gauge bosons, and the change of couplings of the SM particles affect this process.

We have studied the total cross section and the polarization fraction of the W's produced for typical parameter values. We conclude that for suitable choice of beam polarizations, there can be more than 50% deviation in the cross section for $\sqrt{s}$ around and above $500\,\text{GeV}$. The polarization fractions are found to be more sensitive to the new effects, which can be two or three times the SM value at $\sqrt{s} = 800\,\text{GeV}$. The fact that the W polarization fractions can be very precisely measured at ILC shows that study of these observables can effectively probe the LHM.

Study of secondary lepton distributions can be carried out efficiently at the ILC. Our study of the energy and angular distributions in the laboratory frame shows that significant deviation from the SM expectation is possible for parameter sets of LHM allowed by the present experimental constraints. We see that the angular distribution is better suited in the present case with fraction of secondary leptons emitted in the backward direction deviates from the SM value by significant amounts. We have introduced a LR asymmetry for the differential as well as the integrated cases, where the integration is performed over an opening angle given by θ_0. It is shown that a judicious choice of θ_0 can provide a window for observing striking deviations from the SM and provide a discriminating tool for the LHM.

While a more complete study including, for instance, detector efficiencies, and larger parameter space scan is pending, our study with representative parameter points illustrates that W pair production in e^+e^- collisions at ILC energies can probe the LHM very effectively.

Acknowledgments

A $A(s, x, \theta_l)$

The expression for energy-angle correlation for the unpolarised beams is given in ref. [14, 15], for the SM and for the BESS models respectively, which may be easily adapted for the LHM. The generalization to include arbitary beam polarization for each of these models can also be done in a straightforward manner. Here we give it for the LHM. The expressions result from straightforward Dirac trace techniques to include longitudinal beam polarization, by evalauting the electronic part of the Feynman diagrams given in figure 1. In particular, for C_s and C'_s the requisite traces which produce the beam polarization dependence associated with them are analogous to those that have been explicitly discussed in ref. [16]. The beam polarization dependence in C_{int} and C_t which we have presented explicitly here, reflect the maximal parity violating nature of the couplings of the Ws to the electrons and positrons in the t-channel diagram.

For arbitrary beam we have $A(s, x, \theta_l) = C_s A_s + C'_s A'_s + C_{\text{int}} A_{\text{int}} + C_t A_t$, with

$$A_s = -\frac{3}{2} - \tau - \frac{\tau}{x} + \frac{\tau^2}{x^2} + \frac{x}{\tau}(1-x)\left(1 + \frac{1}{4\tau}\right)$$
$$+ \left(-\frac{5}{2} - \tau + 3\frac{\tau}{x} - 3\frac{\tau^2}{x^2} + \frac{1}{2\tau} + \frac{x}{\tau}(1-x)\left(1 - \frac{1}{4\tau}\right)\right)\cos^2\theta_l,$$

$$A'_s = 2\left(1 + \frac{1}{4\tau} - 2x - 2\frac{\tau}{x}\right)\cos\theta_l,$$

$$A_{\text{int}} = -2\tau + \frac{x}{\tau} - 2 + \frac{x}{2\tau}(1-x)\left(1 + \frac{1}{2\tau}\right) + \left(1 + \frac{1}{2\tau} - \frac{2\tau}{x} - 2x\right)\cos\theta_l$$
$$- \left(1 - \frac{1}{2\tau}\right)\left(1 - \frac{x(1-x)}{2\tau}\right)\cos^2\theta_l$$
$$- Rx^2\left(2 + (\cos\theta_l - \beta\cos\theta) \times \left(2 - \left(1 + \frac{1}{\tau}\right)\beta\cos\theta + \cos\theta_l\right)\right),$$

$$A_t = \left(-2 + \frac{2x}{\tau} + \frac{x(1-x)}{4\tau^2}\right) + \frac{\cos\theta_l}{2\tau} + \left(1 - (1-x)\frac{x}{2\tau}\right)\frac{\cos^2\theta_l}{2\tau}$$
$$- \frac{2}{\tau}x^2 R(\beta\cos\theta - \cos\theta_l)\beta\cos\theta + 2x^2 a R^3(\beta\cos\theta - \cos\theta_l)^2.$$

Here

$$R = \left[4\tau^2 + (\beta\cos\theta - \cos\theta_l)(\beta\cos\theta - \beta^2\cos\theta_l)\right]^{-\frac{1}{2}}$$
$$a = 2\tau - 1 + \beta\cos\theta\cos\theta_l,$$

where $\cos\theta = 1/\beta\,(1 - 2\tau/x)$ is the scattering angle of W^- and $\beta = (1 - 4m_W^2/s)^{\frac{1}{2}}$ is the velocity of W^-, both in the centre of mass frame. The coefficients, C's are given below for arbitrary beam polarizations with P_{e^-} and P_{e^+} denoting the degrees of electron and positron beams, respectively. In addition to the standard channels (as given in ref. [14, 15]),

these coefficients include the contribution due the Z_H exchange.

$$C_s = (1 - P_{e^-}P_{e^+}) \ \left(g_{\gamma WW}^2 \left[(c_\gamma^v)^2 + (c_\gamma^a)^2 - P \ (2c_\gamma^a c_\gamma^v) \right] \right.$$
$$+ s_Z^2 \ g_{\mathrm{ZWW}}^2 \ \left[(c_Z^v)^2 + (c_Z^a)^2 - P \ (2c_Z^a c_Z^v) \right]$$
$$+ s_{Z_H}^2 \ g_{Z_H WW}^2 \ \left[(c_{Z_H}^v)^2 + (c_{Z_H}^a)^2 - P \ (2c_{Z_H}^a c_{Z_H}^v) \right]$$
$$+ 2 \ s_Z \ g_{\gamma WW} \ g_{\mathrm{ZWW}} \ \left[c_\gamma^v c_Z^v + c_\gamma^a c_Z^a - P \ (c_\gamma^a c_Z^v + c_Z^a c_\gamma^v) \right]$$
$$+ 2 \ s_{Z_H} \ g_{\gamma WW} \ g_{Z_H WW} \ \left[c_\gamma^v c_{Z_H}^v + c_\gamma^a c_{Z_H}^a - P \ (c_\gamma^a c_{Z_H}^v + c_{Z_H}^a c_\gamma^v) \right]$$
$$\left. + 2 \ s_Z \ s_{Z_H} \ g_{\mathrm{ZWW}} \ g_{Z_H WW} \ \left[c_Z^v c_{Z_H}^v + c_Z^a c_{Z_H}^a - P \ (c_Z^a c_{Z_H}^v + c_{Z_H}^a c_Z^v) \right] \right)$$

$$C_s' = (1 - P_{e^-}P_{e^+}) \ \left(g_{\gamma WW}^2 \left[2c_\gamma^a c_\gamma^v - P \ ((c_\gamma^v)^2 + (c_\gamma^a)^2) \right] \right.$$
$$+ s_Z^2 \ g_{\mathrm{ZWW}}^2 \ \left[2c_Z^a c_Z^v - P((c_Z^v)^2 + (c_Z^a)^2) \right]$$
$$+ s_{Z_H}^2 \ g_{Z_H WW}^2 \ \left[2c_{Z_H}^a c_{Z_H}^v - P \ ((c_{Z_H}^v)^2 + (c_{Z_H}^a)^2) \right]$$
$$+ 2 \ s_Z \ g_{\gamma WW} \ g_{\mathrm{ZWW}} \ \left[(c_Z^a c_\gamma^v + c_\gamma^a c_Z^v) - P \ (c_\gamma^v c_Z^v + c_\gamma^a c_Z^a) \right]$$
$$+ 2 \ s_{Z_H} \ g_{\gamma WW} \ g_{Z_H WW} \ \left[(c_{Z_H}^a c_\gamma^v + c_\gamma^a c_{Z_H}^v) - P \ (c_\gamma^v c_{Z_H}^v + c_\gamma^a c_{Z_H}^a) \right]$$
$$\left. + 2 \ s_Z \ s_{Z_H} \ g_{Z_H WW} \ g_{\mathrm{ZWW}} \ \left[(c_{Z_H}^a c_Z^v + c_Z^a c_{Z_H}^v) - P \ (c_Z^v c_{Z_H}^v + c_{Z_H}^a c_Z^a) \right] \right)$$

$$C_{\mathrm{int}} = g_{e\nu W}^2 \ \left(g_{\gamma WW} \ (c_\gamma^v + c_\gamma^a) + s_Z \ g_{\mathrm{ZWW}} \ (c_Z^v + c_Z^a) + s_{Z_H} \ g_{Z_H WW} \ (c_{Z_H}^v + c_{Z_H}^a) \right)$$
$$\times (1 - P_{e^-})(1 + P_{e^+})$$

$$C_t = \frac{g_{e\nu W}^4}{2} \times (1 - P_{e^-})(1 + P_{e^+})$$

Here, the effective polarization, $P = (P_{e^-} - P_{e^+})/(1 - P_{e^-}P_{e^+})$, and the propagator factors are defined as: $s_V = s/(s - m_V^2)$, where m_V is the mass of the corresponding gauge boson, $V = Z, \ Z_H$. We have assumed that the centre of mass energy is sufficiently far away from the threshold regions of the gauge bosons involved.

References

[1] K. Hagiwara, R.D. Peccei, D. Zeppenfeld and K. Hikasa, *Probing the weak boson sector in* $e^+e^- \to W^+W^-$, *Nucl. Phys.* **B 282** (1987) 253 [SPIRES].

[2] G. Gounaris, J. Layssac, G. Moultaka and F.M. Renard, *Analytic expressions of cross-sections, asymmetries and W density matrices for* $e^+e^- \to W^+W^-$ *with general three boson couplings*, *Int. J. Mod. Phys.* **A 8** (1993) 3285 [SPIRES].

[3] N. Arkani-Hamed, A.G. Cohen, T. Gregoire and J.G. Wacker, *Phenomenology of electroweak symmetry breaking from theory space*, *JHEP* **08** (2002) 020 [hep-ph/0202089] [SPIRES];
N. Arkani-Hamed et al., *The minimal Moose for a Little Higgs*, *JHEP* **08** (2002) 021 [hep-ph/0206020] [SPIRES].

[4] N. Arkani-Hamed, A.G. Cohen, E. Katz and A.E. Nelson, *The littlest Higgs*, *JHEP* **07** (2002) 034 [hep-ph/0206021] [SPIRES];
M. Schmaltz and D. Tucker-Smith, *Little Higgs review*, *Ann. Rev. Nucl. Part. Sci.* **55** (2005) 229 [hep-ph/0502182] [SPIRES];
M. Perelstein, *Little Higgs models and their phenomenology*, *Prog. Part. Nucl. Phys.* **58** (2007) 247 [hep-ph/0512128] [SPIRES].

[5] P. Poulose, *Littlest Higgs model and W pair production at international linear collider*, *Pramana* **69** (2007) 909 [SPIRES].

[6] G.A. Moortgat-Pick et al., *The role of polarized positrons and electrons in revealing fundamental interactions at the linear collider*, *Phys. Rept.* **460** (2008) 131 [hep-ph/0507011] [SPIRES].

[7] M. Perelstein, M.E. Peskin and A. Pierce, *Top quarks and electroweak symmetry breaking in little Higgs models*, *Phys. Rev.* **D 69** (2004) 075002 [hep-ph/0310039] [SPIRES].

[8] C. Csáki, J. Hubisz, G.D. Kribs, P. Meade and J. Terning, *Variations of little Higgs models and their electroweak constraints*, *Phys. Rev.* **D 68** (2003) 035009 [hep-ph/0303236] [SPIRES].

[9] T. Han, H.E. Logan, B. McElrath and L.-T. Wang, *Phenomenology of the little Higgs model*, *Phys. Rev.* **D 67** (2003) 095004 [hep-ph/0301040] [SPIRES]; *Loop induced decays of the little Higgs: $h \to gg, \gamma\gamma$*, *Phys. Lett.* **B 563** (2003) 191 [*Erratum ibid.* **B 603** (2004) 257] [hep-ph/0302188] [SPIRES];
T. Han, H.E. Logan and L.-T. Wang, *Smoking-gun signatures of little Higgs models*, *JHEP* **01** (2006) 099 [hep-ph/0506313] [SPIRES];
J.A. Conley, J.L. Hewett and M.P. Le, *Determination of Littlest Higgs model parameters at the ILC*, *Phys. Rev.* **D 72** (2005) 115014 [hep-ph/0507198] [SPIRES];
Y.-B. Liu, L.-L. Du and X.-L. Wang, *Higgs boson pair production process $e^+e^- \to ZHH$ in the littlest Higgs model at the ILC*, *J. Phys.* **G 33** (2007) 577 [hep-ph/0609208] [SPIRES];
W. Kilian, D. Rainwater and J. Reuter, *Distinguishing Little-Higgs product and simple group models at the LHC and ILC*, *Phys. Rev.* **D 74** (2006) 095003 [hep-ph/0609119] [SPIRES];
E. Asakawa et al., *Precision measurements of Little Higgs parameters at the International Linear Collider*, *Phys. Rev.* **D 79** (2009) 075013 [arXiv:0901.1081] [SPIRES];
S. Yang, *Associated production of the Higgs boson and a single top quark in the littlest Higgs model at Large Hadron Collier*, arXiv:0904.1646 [SPIRES];
A. Dobado, L. Tabares-Cheluci, S. Penaranda and J.R. Laguna, *Radiative corrections to the Higgs potential in the LH model*, arXiv:0907.1483 [SPIRES].

[10] C. Csáki, J. Hubisz, G.D. Kribs, P. Meade and J. Terning, *Big corrections from a little Higgs*, *Phys. Rev.* **D 67** (2003) 115002 [hep-ph/0211124] [SPIRES].

[11] A. Dobado, L. Tabares-Cheluci and S. Penaranda, *The Higgs effective potential in the littlest Higgs model at the one-loop level*, *Phys. Rev.* **D 75** (2007) 083527 [hep-ph/0612131] [SPIRES].

[12] A.A. Pankov and N. Paver, *Initial longitudinal polarization in $e^+e^- \to W^+W^-$ as a tool to probe trilinear gauge boson couplings*, *Phys. Lett.* **B 324** (1994) 224 [SPIRES].

[13] L3 collaboration, M. Acciarri et al., *Direct observation of longitudinally polarized $W^\pm$ bosons*, *Phys. Lett.* **B 474** (2000) 194 [hep-ex/0001016] [SPIRES].

[14] V.A. Kovalchuk, M.P. Rekalo and I.V. Stoletnyi, *The muon spectra from decays of W and Z bosons produced in e^+e^- collisions*, *Z. Phys.* **C 23** (1984) 111 [SPIRES].

[15] P. Poulose, S.D. Rindani and L.M. Sehgal, *Lepton spectra from $e^+e^- \to W+ W-$ in the BESS model*, *Phys. Lett.* **B 525** (2002) 71 [hep-ph/0111134] [SPIRES].

[16] B. Ananthanarayan and S.D. Rindani, *Weak dipole moment of tau in e^+e^- collisions with longitudinally polarized electrons*, *Phys. Rev. Lett.* **73** (1994) 1215 [hep-ph/9310312] [SPIRES]; *Effect of longitudinal electron polarization in the measurement of the tau weak dipole moment in e^+e^- collisions*, *Phys. Rev.* **D 50** (1994) 4447 [hep-ph/9403346] [SPIRES]; *Measurement of the tau electric dipole moment using longitudinal polarization of e^+e^- beams*, *Phys. Rev.* **D 51** (1995) 5996 [hep-ph/9411399] [SPIRES].